Frequency Tuning of the Linearly and Circularly Polarized Dielectric Resonator Antennas Using Multiple Parasitic Strips

Hoi Kuen Ng, *Member, IEEE*, and Kwok Wa Leung, *Senior Member, IEEE*

***Abstract*—A rigorous analysis of the conformal-strip-excited hemispherical dielectric resonator antenna (DRA) with multiple parasitic strips is presented in this paper. The problem is formulated using the Green's function approach, with the strip currents solved by using the method of moments. It is found that the strips can be used to tune the operating frequency of both the linearly polarized (LP) and circularly polarized (CP) DRAs. In designing the LP DRA, the parasitic strips are placed symmetrically in pairs to minimize cross-polarized radiation fields. For the CP DRA, however, the parasitic strips are asymmetric, with their parameters determined by using the Genetic Algorithm. Measurements were carried out to verify the calculations, and reasonable agreement between theory and experiment is obtained.**

***Index Terms*—Dielectric antennas, frequency tuning, method of moments (MoM), parasitic antennas.**

I. Introduction

The dielectric resonator antenna (DRA) [1] has received much attention in the last two decades [2]–[17]. The DRA can be fabricated from a low-loss and temperature-stable dielectric material, with a number of advantages such as its small size, low cost, lightweight, and ease of excitation.

The resonant frequency of the DRA is determined by the physical dimensions and dielectric constant. Unfortunately, the DRA for a particular frequency may not be available from the commercial market. Even if a suitable DRA can be obtained, the measured and calculated resonant frequencies are usually different from each other due to fabrication tolerances. Therefore, some post-manufacturing frequency-tuning methods were studied for the linearly polarized (LP) DRA. Li *et al.* [7] and Chen *et al.* [8] experimentally tuned the DRA frequency by using a conductive loading disk. Recently, the loading-disk method has been studied theoretically and experimentally [9]. In this paper, the tunable frequency range in [9] is extended by using a pair of parasitic strips. The new approach provides more degrees of freedom than the loading-disk method. It is found that the tunable frequency range can be extended even further if more parasitic strips are used. To demonstrate the new method, the conformal-strip [10], [11] fed hemispherical DRA excited in its fundamental TE_{111} mode is used. The conformal excitation scheme shares the advantages of the probe-feed method, but it desirably eliminates the necessity to drill a hole for the probe penetration. Since the excitation strip is conformal to the curved surface, the strip can be mounted on the DRA perfectly without creating any air gaps. Moreover, the strip length can be adjusted easily for post-manufacturing trimmings, and reduction of the lengths can be made by simply removing some of the metallization.

In the last decade, significant effort has been paid to the circularly polarized (CP) DRA [12]–[15] because, as compared with the linearly polarized (LP) system, the CP system allows more flexible orientations between the transmitting and receiving antennas. Moreover, CP fields are less sensitive to the propagation effect than LP fields, making the CP system very suitable for satellite communications. Recently, a conformal-strip fed CP DRA with a single parasitic strip was studied [14], [15], but it was found that its CP operating frequency cannot be tuned easily [15]. In this paper, the multiple-parasitic-strip method is used to tune the CP frequency. It should be mentioned that although the previous parasitic-slot method [16], [17] is able to tune both the LP and CP frequencies, it was for the design stage only. In contrast, the proposed method is suitable for both the design stage and post-manufacturing tuning.

For the CP part, the genetic algorithm (GA) [18] is used to facilitate the design. The GA is a universal optimization tool that searches over the complete solution domain using the principles of natural selection and survival of the fitness. Unlike the gradient search, the GA is a robust and stochastic search method even for a very complicated objective function. Recently, the usefulness of the GA was illustrated through the design of a CP microstrip antenna [19], with the axial ratio (AR) and input impedance optimized by the GA. In this paper, the GA is employed to optimize the AR and return loss by selecting different strip lengths and positions.

It is worth mentioning that although the hemispherical shape is not the most practical one, knowledge of the hemispherical DRA can be applied to other DRAs such as the cylindrical and rectangular DRAs. For example, the positions of the parasitic patches for designing CP hemispherical and cylindrical DRAs were found to be around each other; they were 157° and 135° for the hemispherical [15] and cylindrical [14] DRAs, respectively. Confirming the feasibility of this parasitic-patch technique for the hemispherical DRA, the rectangular DRA version was also designed successfully [22].

Academically, the result of the hemispherical DRA can be used to verify the accuracy of various numerical methods. For

Manuscript received February 1, 2005; revised August 12, 2005. This work was supported by a grant from the Research Grant Council of the Hong Kong SAR Project No.: CityU 1178/01E.

The authors are with the Wireless Communications Research Centre and Department of Electronic Engineering, City University of Hong Kong, Kowloon, Hong Kong (e-mail: hkng@ee.cityu.edu.hk).

Digital Object Identifier 10.1109/TAP.2005.861546

0018-926X/$20.00 © 2006 IEEE

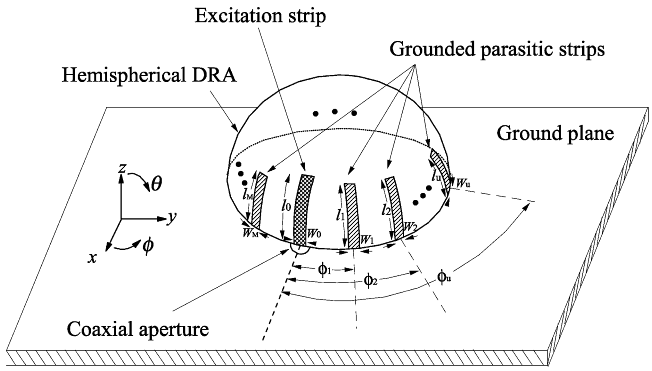

Fig. 1. Configuration of the conformal-strip excited DRA with multiple parasitic strips.

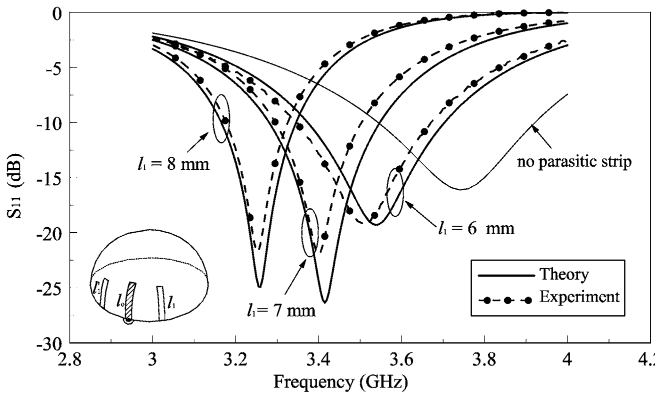

Fig. 2. Measured and calculated S_{11} as a function of frequency for $l_1 = l_1' = 0$, 6.0, 7.0, and 8.0 mm: $a = 12.5$ mm, $\varepsilon_r = 9.5$, $l_0 = 11$ mm, $W_0 = W_1 = W_1' = 1.2$ mm, $\phi_1 = 30°$ and $\phi_1' = 330°$.

instance, the result of the previous probe-fed hemispherical DRA [23] was used by the commercial software package Fidelity [24] to substantiate the validity of the software package.

In this paper, the mode-matching method is used to obtain the Green's functions, which are used to formulate the coupled integral equations for the feeding and parasitic strips. The currents are solved using the method of moments (MoM) with piecewise sinusoidal (PWS) basis functions. Slender strips are used to simplify the problem. The MoM impedance integrals are efficiently evaluated using recurrence formulas [15]. This approach also avoids the singularity problem of the Green functions and therefore greatly facilitates the numerical implementation. For each of the LP and CP parts, measurements were carried out to verify the calculations, and good agreement between theory and experiment is obtained.

II. Theory

The antenna configuration is shown in Fig. 1, where a hemispherical DRA of radius a and dielectric constant ϵ_r is fed by a conformal strip of length l_0 and width W_0. There are M parasitic strips, each of them has length l_u, width W_u, and angular position ϕ_u, where $u = 1, 2, \ldots, M$. In the following formulation, the fields are assumed to vary harmonically as $e^{j\omega t}$. Assuming an infinite ground plane, the strip lengths and DRA size are doubled by using image theory. Since slender strips are used, the currents can be assumed to flow along the $\hat{\theta}$-direction only.

Using the MoM, the uth strip current can be expanded using PWS basis functions as follows:

$$J_{u\theta}(\theta) = \frac{1}{W_u} \sum_{p_u=1}^{N_u} I_{p_u} f_{p_u}(\theta), p_u = 0, 1, 2 \ldots, N_u \quad (1)$$

where N_u is the number of the PWS basis functions $f_{p_u}(\theta)$, which was defined in (3) of [15] with different symbols. It can be proved that by using the Galerkin's technique, the strip currents can be found by solving the following matrix equation:

$$\begin{bmatrix} [Z_{00}] & [Z_{10}] & \cdots & [Z_{M0}] \\ [Z_{01}] & \cdots & \cdots & \vdots \\ \vdots & \vdots & \vdots & \vdots \\ [Z_{0M}] & \cdots & \cdots & [Z_{MM}] \end{bmatrix} \begin{bmatrix} [I_{p_0}] \\ [I_{p_1}] \\ \vdots \\ [I_{p_M}] \end{bmatrix} = \begin{bmatrix} [V_{q_0}] \\ [V_{q_1}] \\ \vdots \\ [V_{q_M}] \end{bmatrix} \quad (2)$$

where

$$Z_{uv} = \frac{-1}{W_u W_v} \int\int_{S=S_t} \int\int_{S'=S_u} f_{q_v}(\theta) G_{J_\theta}^{E_\theta} f_{p_u}(\theta') dS' dS$$
$$u, v = 0, 1, 2, \ldots, M \quad (3)$$

and

$$V_{q_v} = \int_{\pi/2 - l_u/a}^{\pi/2 + l_u/a} f_{q_v}(\theta) \delta(\theta) d\theta$$
$$q = 1, 2, \ldots, N_v \text{ and } v = 0, 1, 2, \ldots, M \quad (4)$$

in which $G_{J_\theta}^{E_\theta}$ is the Green's function of E_θ due to a point current J_θ. The voltage elements of $[V_{q_v}]$ are all zero except $v = 0$ because only the feeding strip has the impressed field. After the strip currents are found, the input impedance of the imaged DRA can be calculated easily as $Z_{\text{in}} = 1/\sum_{p_0=1}^{N_0} I_{p_0} f_{p_0}(0)$. Dividing Z_{in} by 2 gives the input impedance of the original hemispherical configuration. It is worth mentioning that since the integrals Z_{uv} (3) can be evaluated easily by using recurrence formulas [15], no numerical integration is required to calculate the input impedance. From the strip currents, the far field of the antenna can also be obtained easily.

III. Measured and Calculated Results

A. LP DRA

To verify the theory, a hemispherical DRA of radius $a = 12.5$ mm and dielectric constant $\epsilon_{\text{ra}} = 9.5$ was measured using an HP8510C network analyzer. The excitation strip has length $l_0 = 11.0$ mm. Two identical grounded parasitic strips of length $l_1 = l_1'$ are cut from a conducting adhesive tape. To minimize the cross polarized fields, the two parasitic strips are placed symmetrically at angular positions ϕ_1 and $\phi_1' = 360° - \phi_1$. The widths of all the feeding and parasitic strips are 1.2 mm. To reduce errors introduced by possible air gaps [20] between the ground plane and DRA, the previous experimental technique [10] was used. A conducting tape of size larger than the base of the DRA was cut. Then the DRA was put on the adhesive side of the conducting tape. Additional adhesive tapes were used to mount the DRA-attached tape on the ground plane of size 30×30 cm. Since the conducting tape was adhered to the base of the DRA comformally, the air gap was removed. The measured and calculated S_{11} as a function of frequency for $l_1 = l_1' = 0$, 6.0, 7.0, and 8.0 mm are shown in Fig. 2, with

TABLE I
FREQUENCY TUNING OF THE DRA USING DIFFERENT STRIP LENGTHS AND POSITIONS. PLEASE REFER TO THE DRAWING IN FIG. 5 FOR THE DEFINITIONS OF THE SYMBOLS l_1, l_1', l_2, AND l_2'

$l_1 = l_1'$ (mm)	ϕ_1 ($\phi_1'=2\pi-\phi_1$)	$l_2 = l_2'$ (mm)	ϕ_2 ($\phi_2'=2\pi-\phi_2$)	Operating frequency f_{LP} (GHz)	S_{11} at f_{LP} (dB)	Impedance Bandwidth (%) ($S_{11} < -10$dB)
10.3	35°	9.5	155°	2.8	–20.0	3.0
8.6	40°	9.6	160°	2.9	–22.9	3.6
8.6	40°	9.0	160°	3.0	–31.5	4.3
9.2	34°	–	–	3.1	–23.3	3.8
8.7	34°	–	–	3.2	–27.6	4.3
8.2	34°	–	–	3.3	–21.4	4.9
7.8	34°	–	–	3.4	–23.5	5.3
7.3	34°	–	–	3.5	–22.9	5.8
6.8	35°	–	–	3.6	–25.4	6.4
6.3	35°	–	–	3.7	–24.6	6.8
5.7	40°	–	–	3.8	–20.5	6.8
10.7	38°	6.5	160°	3.9	–21.9	3.0
10.2	38°	6.1	160°	4.0	–23.8	3.0
10.0	34°	5.7	155°	4.1	–23.5	3.0

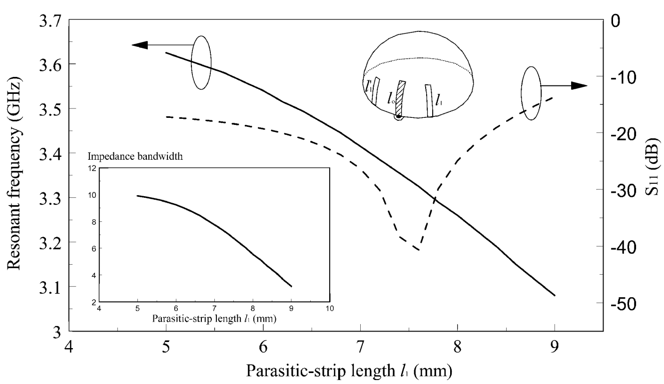

Fig. 3. Measured and calculated resonant frequencies and corresponding $|S_{11}|$ as a function of l_1. Only one pair of parasitic strips are used: $a = 12.5$ mm, $\varepsilon_r = 9.5, l_0 = 14$ mm, $W_0 = W_1 = W_1' = 1.2$ mm, $\phi_1 = 30°$ and $\phi_1' = 330°$.

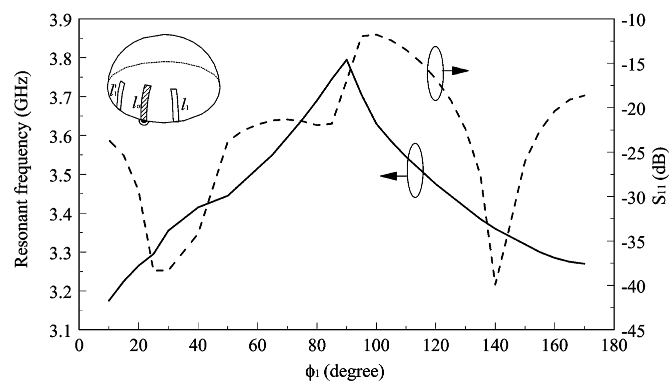

Fig. 4. Calculated resonant frequency and the corresponding $|S_{11}|$ as a function of ϕ_1. Only one pair of parasitic strips are used: $a = 12.5$ mm, $\varepsilon_r = 9.5, l_0 = 14$ mm, $W_0 = W_1 = W_1' = 1.2$ mm, $l_1 = l_1' = 7.4$ mm, and $\phi_1' = 360° - \phi_1$.

angular positions $\phi_1 = 30°$ and $\phi_1' = 330°$. With reference to the figure, good agreement between theory and experiment is observed. The calculated resonant frequencies (minimum S_{11}) are 3.26, 3.4, and 3.54 GHz for $l_1 = l_1' = 6.0$, 7.0, 8.0 mm, respectively, with $S_{11} < -15$ dB. Obviously, the resonant frequency can be tuned lower (resonant frequency for no parasitic strips $= 3.62$ GHz) by adding the length l_1 of the parasitic strips.

The above tunable frequency range can be extended by adding the second pair of parasitic strips of identical length $l_2 = l_2'$. Table I shows the results for $l_0 = 14$ mm, along with other one-pair results. With reference to Table I, the one-pair frequency range is 3.1–3.8 GHz, which is wider than the previous range of 3.25–3.68 GHz obtained using the loading disk method [9]. The frequency range can be extended to 2.8–4.1 GHz by adding the second strip pair. It is noted that the impedance bandwidth is widest around the calculated natural (source-free) resonant frequency (3.7 GHz) of the DRA without any parasitic strips [21]. In this case, the match point is around the peak of the input resistance. However, when the operating frequency increases or decreases, the match point will shift away from the peak and the bandwidth will decrease.

In the following discussions, only one pair of parasitic strips are used unless otherwise stated. Fig. 3 shows the resonant frequency and its corresponding S_{11} as a function of l_1, with $\phi_1 = 30°$. As can be observed from the figure, the resonant frequency decreases from 3.61 to 3.05 GHz by increasing l_1 from 5 mm to 9 mm. Excellent impedance match $(S_{11} < -20\,\text{dB})$ is observed for $6 < l_1 < 8.3$ mm, causing a large dip around $l_1 = 7.5$ mm. For other l_1, the return loss is more than 15 dB, which is acceptable for engineering applications. The inset shows the corresponding impedance bandwidth $(S_{11} < -10\,\text{dB})$. From the figure, it shows that the bandwidth increases with decreasing the lengths of the parasitic strips. The bandwidth of 9.9% is found for $l_1 = 5.5$ mm, which is close to the maximum bandwidth (10.4%) of a simple strip-fed DRA.

Fig. 4 shows the resonant frequency and its corresponding $|S_{11}|$ as a function of ϕ_1, with $l_1 = 7.4$ mm. With reference to the figure, the maximum frequency of 3.8 GHz is obtained when $\phi_1 = 90°$. The return loss is more than 15 dB, except for the region $95° < \phi_1 < 115°$ where the minimum return loss is 10 dB.

We have previously shown that the second pair of parasitic strips can be used to extend the tunable frequency range. The

TABLE II
THE USE OF THE SECOND STRIP PAIR FOR IMPROVING THE RETURN LOSS

Lengths of first pair of parasitic strips	One pair is used at $\phi_1 = 30^\circ$ and $\phi_1' = 330^\circ$		Second pair is added $l_2 = l_2' = 7.6$ mm $\phi_2 = 80^\circ$ and $\phi_2' = 280^\circ$	
$l_1 = l_1'$ (mm)	Operated freq. f_{LP} (GHz)	S_{11} at f_{LP} (dB)	Operated freq. f_{LP} (GHz)	S_{11} at f_{LP} (dB)
5.00	3.625	–17.1851	3.625	–72.4480
5.20	3.610	–17.4568	3.615	–40.9451
5.40	3.595	–17.7885	3.600	–36.5888
5.60	3.580	–18.1887	3.580	–33.8507
5.80	3.560	–18.6837	3.565	–32.2838
6.00	3.540	–19.2918	3.540	–31.6317
6.20	3.515	–20.0487	3.520	–31.7442
6.40	3.495	–21.0180	3.495	–32.6376
6.60	3.470	–22.2693	3.470	–34.5724
6.80	3.440	–23.9267	3.440	–38.8646

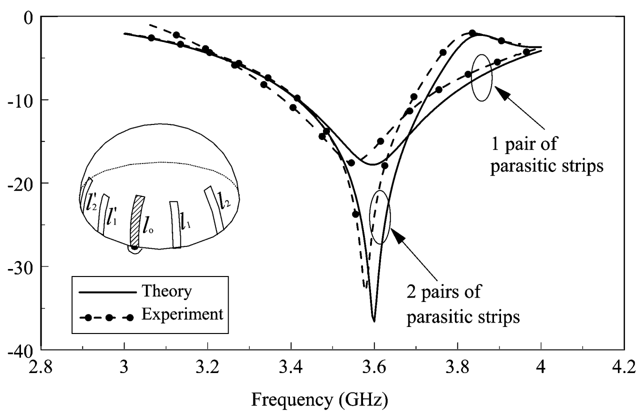

Fig. 5. Measured and calculated S_{11} as a function of frequency for using different numbers of strip pairs: $a = 12.5$ mm, $\varepsilon_r = 9.5$, $l_0 = 14$ mm, $W_0 = W_1 = W_1' = 1.2$ mm. (i) One pair of parasitic strips: $l_1 = l_1' = 5.4$ mm and $\phi_1 = 30^\circ$ and $\phi_1' = 330^\circ$. (ii) Two pairs of parasitic strips: $l_1 = l_1' = 5.4$ mm, $\phi_1 = 30^\circ$, $\phi_1' = 330^\circ$, $l_2 = l_2' = 7.6$ mm, $W_2 = W_2' = 1.2$ mm, $\phi_2 = 80^\circ$, and $\phi_2' = 280^\circ$.

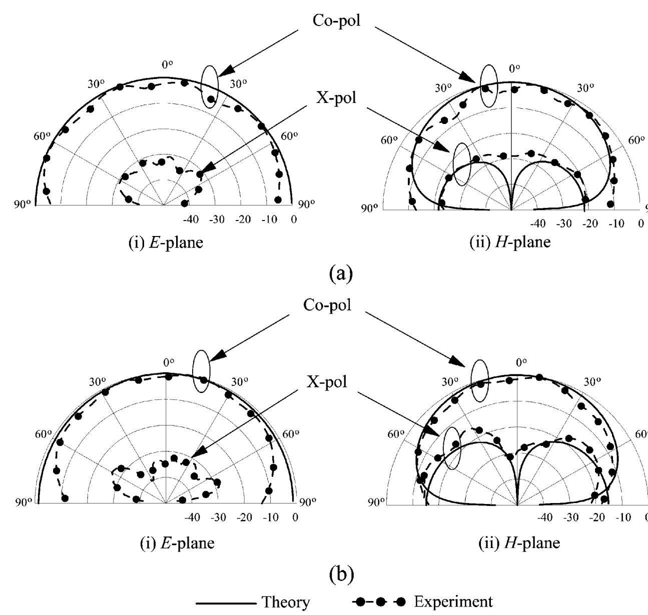

Fig. 6. Measured and calculated co- and cross-polarized field patterns at 3.6 GHz for using different numbers of parasitic strips. (a) One pair of parasitic strips: $a = 12.5$ mm, $\varepsilon_r = 9.5$, $l_0 = 14$ mm, $W_0 = W_1 = W_1' = 1.2$ mm, $l_1 = l_1' = 5.4$ mm, $\phi_1 = 30^\circ$ and $\phi_1' = 330^\circ$. (b) Two pairs of parasitic strip: $l_2 = l_2' = 7.6$ mm, $W_2 = W_2' = 1.2$ mm, $\phi_2 = 80^\circ$, and $\phi_2' = 280^\circ$. The first-pair parameters are the same as in (a).

second strip pair, in fact, can also be used to improve the impedance match with virtually no effects on the resonant frequency. Fig. 5 shows the measured and calculated S_{11} with different pairs of parasitic strips. With reference to the figure, the return loss using a single pair of parasitic strips is about 17 dB, which is increased to more than 30 dB by adding the strip pair of lengths $l_2 = l_2' = 7.6$ mm. Table II shows some other calculated results obtained by the trial and error method. It is interesting to note that the resonant frequency remains almost unchanged when the second pair of parasitic strips is added.

Fig. 6 shows the measured and calculated broadside radiation patterns for the two configurations of Fig. 5. Reasonable agreement between theory and experiment is found, with the discrepancy mainly caused by the finite ground plane effect that the theory has neglected. When there are only one pair of parasitic strips, both the co- and cross-polarized radiation patterns [Fig. 6(a)] are very close to those without the parasitic strips [10]. The cross-polarized fields, however, in general increase after the second pair of parasitic strips are added, as shown in Fig. 6(b). Nevertheless, the calculated cross-polarized fields in the broadside direction $(\theta = 0^\circ)$ still remain vanishingly small in this case.

B. CP DRA

Symmetrical and identical parasitic strips have been used above to minimize the crosspolarized fields. Here, asymmetric parasitic strips are used to excite two nearly orthogonal fields for the generation of CP fields. Since the design involves many parameters, the GA is used to facilitate the design. It was found that although a good AR can be obtained when the two parasitic strips are placed on different sides of the feeding strip, the impedance match is poor. Therefore, the two parasitic strips are placed on the same side. Table III summarizes the results, with the parameters determined by the GA. In optimizing the results, the minimum AR is set to be 1 dB at the optimum AR frequency f_{CP}, and the minimum return loss at f_{CP} is 15 dB. With reference to Table III, f_{CP} can be tuned from 3.2 to 4.1 GHz, with the AR bandwidth $(\mathrm{AR} < -3\,\mathrm{dB}) \sim$ 2–4%. The AR bandwidths obtained within the range are typical for a singly-fed DRA. The maximum AR

TABLE III
THE OPERATING CP FREQUENCY $f_{\rm CP}$, RETURN LOSS AT $f_{\rm CP}$, AND THE AR BANDWIDTH OF THE CP DRA FOR DIFFERENT STRIP PARAMETERS

Feeding strip length	First parasitic strip length		Second parasitic strip length		AR frequency,	S_{11} at f_{CP}	3-dB AR Bandwidth
l_o (mm)	l_1 (mm)	ϕ_1	l_2 (mm)	ϕ_2	f_{CP} (GHz)	(dB)	(%)
13.75	8.70	166.0°	8.86	103.0°	3.20	–16.2	1.9
13.52	7.64	184.0°	8.51	122.5°	3.30	–15.5	2.1
12.63	7.40	171.0°	7.97	121.5°	3.40	–16.3	2.5
13.31	6.73	149.0°	7.54	140.5°	3.50	–15.0	3.0
11.39	12.46	175.0°	7.58	24.5°	3.60	–21.0	3.4
9.77	14.79	155.0°	6.70	22.5°	3.70	–16.5	3.9
11.30	6.03	161.0°	11.86	58.5°	3.80	–16.9	3.1
12.03	4.61	160.0°	9.81	67.5°	3.90	–17.0	2.5
12.24	3.36	154.0°	8.95	78.5°	4.00	–20.2	1.8
8.82	10.06	167.0°	12.44	106.5°	4.10	–17.9	1.8

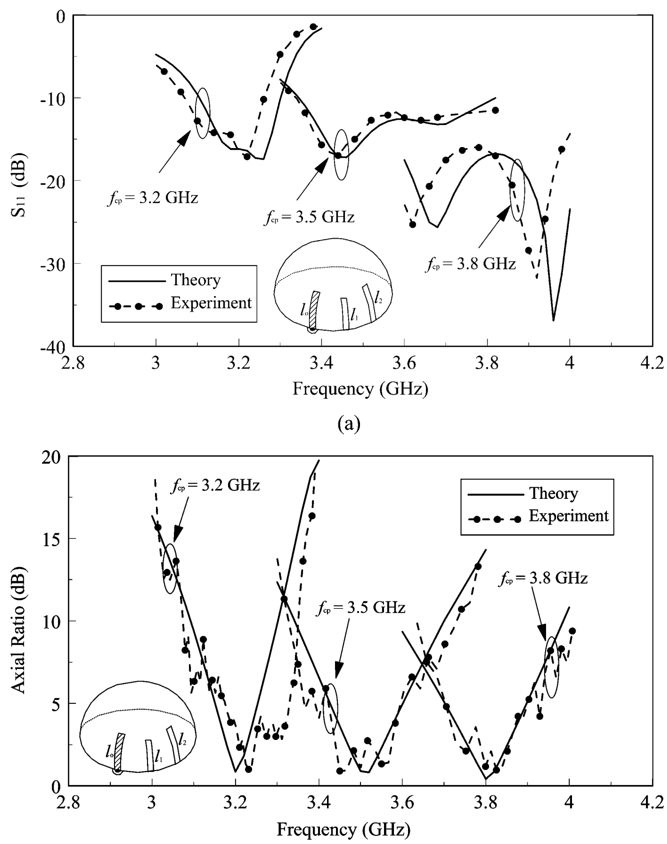

(a) (b)

Fig. 7. Measured and calculated S_{11} and axial ratios as a function of frequency at $f_{\rm CP} = 3.2$, 3.6, and 3.8 GHz: $a = 12.5$ mm, $\varepsilon_r = 9.5$, $W_0 = W_1 = W_2 = 1.2$ mm. Other parameters are given in Table III. (a) Measured and calculated $|S_{11}|$. (b) Measured and calculated axial ratios.

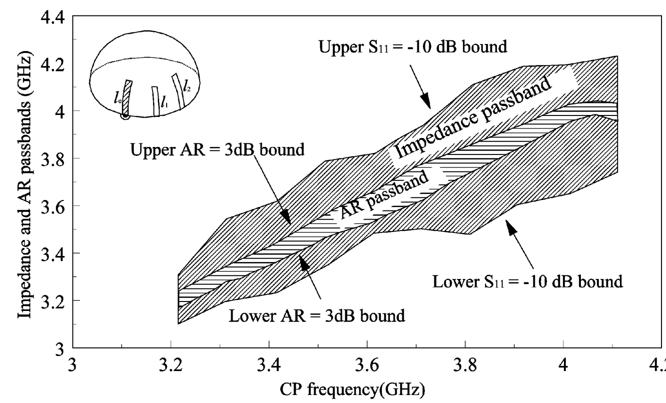

Fig. 8. Impedance and AR passbands as a function of $f_{\rm CP}$: $a = 12.5$ mm, $\varepsilon_r = 9.5$, $W_0 = W_1 = W_2 = 1.2$ mm. Other parameters are given in Table III.

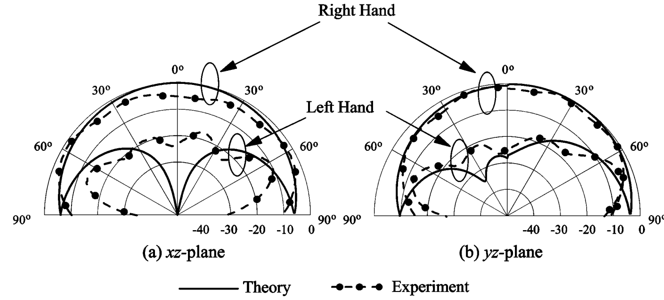

Fig. 9. Measured and calculated right hand and left hand field patterns at $f_{\rm CP} = 3.6$ GHz. Other parameters are given in Table III.

bandwidth (3.9%) is obtained at 3.7 GHz, which is around the natural resonance of the DRA. This bandwidth is significantly wider than the previous AR bandwidth (2.4%) using a single parasitic strip [15].

To verify the calculations, measurements were carried out at $f_{\rm CP} = 3.2$, 3.5 and 3.8 GHz. Fig. 7(a) shows the measured and calculated S_{11}. The calculated S_{11} are -16.2, -15.0 and -21.0 dB for $f_{\rm CP} = 3.2, 3.5,$ and 3.8 GHz, respectively, which satisfy the optimization condition that the return loss has to be at least 15 dB. It was found that the best return loss may not be obtained at $f_{\rm CP}$. The measured and calculated AR's are shown in Fig. 7(b), where the ripples of the measured results are primarily caused by the finite ground plane diffraction.

Fig. 8 shows the impedance and AR passbands as a function of the CP frequency. It is very good that the AR passband overlaps with the impedance passband over the whole tunable frequency range. With reference to the figure, the impedance bandwidth is much wider than the AR bandwidth, and, as usual, the antenna bandwidth is limited by the AR. The reason is that the impedance bandwidth is dependent on the energy loss of the system (including the radiation loss) only. However, the CP operation relies on both the similarity and orthogonality between the two degenerate modes, which cannot be maintained over a wide frequency range using a single feed.

The measured and calculated radiation fields at $f_{\rm CP} = 3.5$ GHz is shown in Fig. 9, where a broadside radiation mode is observed. The DRA is a right-hand (RH) CP antenna. A left-hand (LH) CP antenna can be obtained if the parasitic strips are located on the other side of the feeding strip.

IV. Conclusion

The conformal-strip fed hemispherical DRA with multiple parasitic strips has been studied theoretically and experimentally, with the DRA excited in its fundamental TE_{111} mode. Use has been made of the Green's function method to formulate the problem. The MoM has been employed to solve for the strip currents, from which the input impedance and radiation field of the DRA have been obtained. The calculated results have been substantiated by measurements, and reasonable agreement between theory and experiment has been obtained.

The LP DRA has been studied in the first part of this paper. Parasitic strips of the same length but different angular positions have been added in pairs to minimize the cross-polarized fields. By using a pair of parasitic strip, the tunable frequency range is 3.08–3.80 GHz, which is wider than the previous range of 3.25–3.68 GHz using the loading-disk method. It has been shown that the second pair of parasitic strips can be added to further increase the range to 2.8–4.1 GHz. Apart from increasing the tunable frequency range, the second strip pair can also be used to improve the impedance match.

The CP DRA using a pair of parasitic strips has been studied in the second part of the paper. In this case, the Genetic Algorithm has been employed to facilitate the design. It has been found that a good axial ratio $(\mathrm{AR} < 1\ \mathrm{dB})$ and impedance match $(S_{11} < -15\ \mathrm{dB})$ can easily be obtained inside the tunable frequency range of 3.2–4.1 GHz. The antenna bandwidth is limited by the AR, which has bandwidth of about 2–4% over the tunable frequency range.

Acknowledgment

The constructive comments of the reviewers are gratefully appreciated.

References

[1] S. A. Long, M. W. McAllister, and L. C. Shen, "The resonant cylindrical dielectric cavity antenna," *IEEE Trans. Antennas Propag.*, vol. 31, no. 3, pp. 406–412, May 1983.
[2] K. M. Luk and K. W. Leung, *Dielectric Resonator Antennas*. Baldock, Hertfordshire, U.K.: Research Studies Press, 2003.
[3] A. Petosa, A. Ittipiboon, Y. M. M. Antar, D. Roscoe, and M. Cuhaci, "Recent advances in dielectric-resonator antenna technology," *IEEE Antennas Propag. Mag.*, vol. 40, pp. 35–48, Jun. 1998.
[4] Z. Fan, Y. M. M. Antar, A. Ittipiboon, and A. Petosa, "Parasitic coplanar three-element dielectric resonator antenna subarray," *Electron. Lett.*, vol. 32, pp. 789–790, Apr. 1996.
[5] A. A. Kishk, Y. Yan, and A. W. Glisson, "Conical dielectric resonator antennas for wide-band applications," *IEEE Trans. Antennas Propag.*, vol. 50, no. 4, pp. 469–474, Apr. 2002.
[6] G. P. Junker, A. A. Kishk, and A. W. Glisson, "Input impedance of aperture-coupled dielectric resonator antennas," *IEEE Trans. Antennas Propag.*, vol. 44, no. 5, pp. 600–607, May 1996.
[7] Z. Li, C. Wu, and J. Litva, "Adjustable frequency dielectric resonator antenna," *Electron. Lett.*, vol. 32, pp. 606–607, Mar. 1996.
[8] Z. N. Chen, K. W. Leung, K. M. Luk, and E. K. N. Yung, "Effect of parasitic disk on a coaxial probe-fed dielectric resonator antenna," *Microw. Opt. Techn. Lett.*, vol. 15, pp. 166–168, Jun. 1997.
[9] H. K. Ng and K. W. Leung, "Frequency tuning of the dielectric resonator antenna using a loading cap," *IEEE Trans. Antennas Propag.*, vol. 53, no. 3, pp. 1229–1232, Mar. 2005.
[10] K. W. Leung, "Conformal strip excitation of dielectric resonator antenna," *IEEE Trans. Antennas Propag.*, vol. 48, no. 6, pp. 961–967, Jun. 2000.
[11] M. Copper, "Investigation of Current and Novel Rectangular Dielectric Resonator Antennas for Broadband Applications at L-Band Frequencies," Master's, Carleton University, 1997.
[12] K. P. Esselle, "Circularly polarized higher-order rectangular dielectric resonator antenna," *Electron. Lett.*, vol. 32, pp. 1742–1743, Sep. 1996.
[13] M. T. Lee, K. M. Luk, E. K. N. Yung, and K. W. Leung, "Microstripline feed circularly polarized cylindrical dielectric resonator antenna," *Microw. Opt. Techn. Lett.*, vol. 24, pp. 206–207, Mar. 2000.
[14] R. T. Long, R. J. Dorris, S. A. Long, M. A. Khayat, and J. T. Williams, "Use of parasitic strip to produce circular polarization and increased bandwidth for cylindrical dielectric resonator antenna," *Electron. Lett.*, vol. 37, pp. 406–408, Mar. 2001.
[15] K. W. Leung and H. K. Ng, "Theory and experiment of circularly polarized dielectric resonator antenna with a parasitic patch," *IEEE Trans. Antennas Propag.*, vol. 51, no. 3, pp. 405–412, Mar. 2003.
[16] C. Y. Huang and C. W. Ling, "Frequency-adjustable circularly polarized dielectric resonator antenna with slotted ground plane," *Electron. Lett.*, vol. 39, pp. 1030–1031, Jul. 2003.
[17] K. W. Leung and K. K. So, "Frequency-tunable designs of the linearly and circularly polarized dielectric resonator antennas using a parasitic slot," *IEEE Trans. Antennas Propag.*, vol. 53, no. 1, pp. 572–576, Jan. 2005.
[18] Y. Rahmat-Samii and E. Michielssen, *Electromagnetic Optimization by Genetic Algorithms*. New York: Wiley-Interscience, 1999.
[19] D. Lee and S. Lee, "Design of a coaxially fed circularly polarized rectangular microstrip antenna using a genetic algorithm," *Microw. Opt. Techn. Lett.*, vol. 26, no. 5, pp. 288–291, Sep. 2000.
[20] G. P. Junker, A. A. Kishk, A. W. Glisson, and D. Kajfez, "Effect of fabrication imperfections for ground-plane-backed dielectric resonator antennas," *IEEE Antennas Propag. Mag.*, vol. 37, no. 1, pp. 40–46, 1995.
[21] K. W. Leung, K. M. Luk, K. Y. A. Lai, and D. Lin, "Theory and experiment of an aperture-coupled hemispherical dielectric resonator antenna," *IEEE Trans. Antennas Propag.*, vol. 43, no. 11, pp. 1192–1198, Nov. 1995.
[22] B. Li and K. W. Leung, "Strip-fed rectangular dielectric resonator antenna with/without a parasitic patch," *IEEE Trans. Antennas Propag.*, vol. 53, no. 7, pp. 2200–2207, Jul. 2005.
[23] K. W. Leung, K. M. Luk, K. Y. A. Lai, and D. Lin, "Theory and experiment of a coaxial probe fed dielectric resonator antenna," *IEEE Trans. Antennas Propag.*, vol. 41, no. 10, pp. 1390–1398, Oct. 1993.
[24] Fidelity, Zeland Software, Inc..

Hoi Kuen Ng (S'01–M'05) was born in Hong Kong on April 10, 1975. He received the B.Sc. degree in information technology and the Ph.D. degree in electronic engineering from City University of Hong Kong, Kowloon, Hong Kong, in 1998 and 2003, respectively.

He joined the Department of Electronic Engineering at City University of Hong Kong as a Senior Research Assistant in 2003 and became a Lecturer in 2005. His research interests include dielectric resonator antennas, circularly polarized antennas, and numerical analysis in electromagnetics.

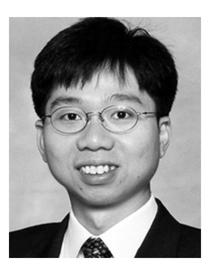

Kwok Wa Leung (S'90–M'93–SM'02) was born in Hong Kong on April 11, 1967. He received the B.Sc. degree in electronics and Ph.D. degree in electronic engineering from the Chinese University of Hong Kong, in 1990 and 1993, respectively.

From 1990 to 1993, he was a Graduate Assistant with the Department of Electronic Engineering, the Chinese University of Hong Kong. In 1994, he joined the Department of Electronic Engineering at City University of Hong Kong, Kowloon, Hong Kong, as an Assistant Professor and became an Associate Professor in 1999. From 2001 to 2004, he was appointed as the Programme Leader for B.Eng. (Honors) in electronic and communication engineering. His research interests include dielectric resonator antennas, microstrip antennas, wire antennas, numerical methods in electromagnetics, and mobile communications.

Dr. Leung received the URSI Young Scientists Awards in 1993 and 1995, awarded by XXIVth General Assembly of the International Union of Radio Science (URSI) and 15th URSI Triennial International Symposium on Electromagnetic Theory, respectively.